



# Histone dynamics play a critical role in SNF2h-mediated nucleosome sliding

Nathan Gamarra<sup>1,2</sup> and Geeta J. Narlikar<sup>1</sup>✉

ARISING FROM: L. Yan et al. *Nat. Struct. Mol. Biol.* <https://doi.org/10.1038/s41594-019-0199-9> (2019)

Elucidating the mechanisms by which ATP-dependent chromatin remodeling enzymes disrupt the structure of the nucleosome is essential to understanding how chromatin states are established and maintained. We have previously demonstrated that dynamics in the histone core are functionally important for nucleosome sliding by the human ISWI-family remodeler SNF2h<sup>1</sup>. Restraining histone octamer dynamics by site-specific disulfide crosslinks engineered in otherwise cysteine-free histones inhibited nucleosome sliding by SNF2h. Using similar approaches, others have also suggested that octamer plasticity is important for nucleosome sliding<sup>2,3</sup>. However, a subsequent study by Chen and colleagues that reported cryo-electron microscopy (cryo-EM) structures of ISWI-family remodeler-nucleosome complexes did not observe stable conformational rearrangements in the histone octamer<sup>4</sup>. The authors of the study were also unable to replicate the finding that restraining histone dynamics by single H3–H4 crosslinks (generated using the mutants H3(L82C) and H4(V81C), and called sCX2) affected nucleosome sliding by SNF2h<sup>1</sup>. Initially, the authors generated sCX2 crosslinks in the background of histone octamers from wild-type *Xenopus laevis*, which bear an endogenous cysteine in histone H3 (H3(C110)). However, the presence of the additional reactive cysteine, which can readily form disulfides under oxidizing conditions<sup>5</sup>, creates the possibility for multiple types of crosslinked species, complicating the interpretation of these results. Yan et al.<sup>4</sup> also created sCX2 crosslinks in an H3(C110A) mutant octamer and, in this case, found that SNF2h sliding activity was impaired, as found by Sinha et al.<sup>1</sup>, but to a lesser extent than previously observed. Furthermore, when the disulfide bond was apparently reduced by adding 100 mM dithiothreitol (DTT) to the nucleosomes, sliding activity was not restored. On the basis of these results, Yan et al. suggested ‘...that the loss of activity did not result from the disulfide bond but probably from non-specific oxidation damage to the nucleosome, which was prone to precipitate out of the solution under the condition of extensive oxidation. Prolonged treatment might have resulted in damage to the nucleosome and loss of the activity’<sup>4</sup>. However, the authors did not directly test this possibility. To address this concern experimentally, we first assembled nucleosomes with cysteine-free *X. laevis* H3(C110A) octamers that were oxidized with copper phenanthroline (Cu-Phe) (Extended Data Fig. 1a). No precipitates were observed during the preparation and the oxidized octamers readily assembled into canonical nucleosomes, suggesting no gross defects. Remodeling of these oxidized nucleosomes with SNF2h after purification by glycerol gradient ultracentrifugation showed no defect compared to nucleosomes assembled from untreated H3(C110A) octamers (Table 1 and Fig. 1a).

To test whether the oxidation method may affect the results in the context of the H3(C110A) sCX2 octamer, we generated H3(C110A) sCX2 crosslinked nucleosomes using Cu-Phe or oxidized glutathione (GSSG), a gentler oxidizing agent that does not generate free radicals and that has previously been used to investigate nucleosome dynamics<sup>6</sup>. Oxidation with Cu-Phe went to near-completion as assessed by a non-reducing SDS–PAGE gel, whereas GSSG oxidation was less efficient (Extended Data Fig. 1a). We then reduced a portion of each H3(C110A) sCX2 crosslinked octamer by dialysis into buffer containing 100 mM DTT (Extended Data Fig. 1b). H3(C110A) sCX2 octamers showed no visible precipitates upon oxidation or after reduction and, like cysteine-free octamers, readily assembled into nucleosome core particles that were purified by glycerol gradient ultracentrifugation. H3(C110A) sCX2 nucleosomes assembled from octamers oxidized with Cu-Phe slowed SNF2h-driven sliding by approximately 40-fold compared with reduced controls under saturating concentrations of SNF2h, whereas nucleosomes assembled from octamers oxidized by GSSG slowed sliding by around 15-fold (Fig. 1b,c). This quantitative difference can be attributed to the different crosslinking efficiencies of the two oxidation protocols and cannot be explained by

**Table 1 | Rate constant ( $k_{\text{obs}}$ ) for nucleosome sliding of the given substrate at different concentrations of SNF2h**

Octamer used to assemble the nucleosome	$k_{\text{obs}}$	
[SNF2h]	1 μM	50 nM
H3(C110A), untreated	$1.6 \pm 0.1 \text{ min}^{-1}$	$0.03 \pm 0.01 \text{ min}^{-1}$
H3(C110A), Cu-Phe oxidized	$1.8 \pm 0.1 \text{ min}^{-1}$	Not determined
H3(C110A), Cu-Phe oxidized and then reduced	$2.3 \pm 0.1 \text{ min}^{-1}$	Not determined
H3(C110A) sCX2, Cu-Phe oxidized	$0.06 \pm 0.03 \text{ min}^{-1}$	Undetectable
H3(C110A) sCX2, Cu-Phe oxidized and then reduced	$2.5 \pm 0.4 \text{ min}^{-1}$	$0.03 \pm 0.02 \text{ min}^{-1}$
H3(C110A) sCX2, GSSG oxidized	$0.14 \pm 0.02 \text{ min}^{-1}$	Not determined
H3(C110A) sCX2, GSSG oxidized and then reduced	$2.2 \pm 0.6 \text{ min}^{-1}$	Not determined

The buffer conditions used have been described previously<sup>1</sup>.

<sup>1</sup>Department of Biochemistry and Biophysics, University of California, San Francisco, San Francisco, CA, USA. <sup>2</sup>TETRAD Graduate Program, University of California, San Francisco, San Francisco, CA, USA. ✉e-mail: [geeta.narlikar@ucsf.edu](mailto:geeta.narlikar@ucsf.edu)

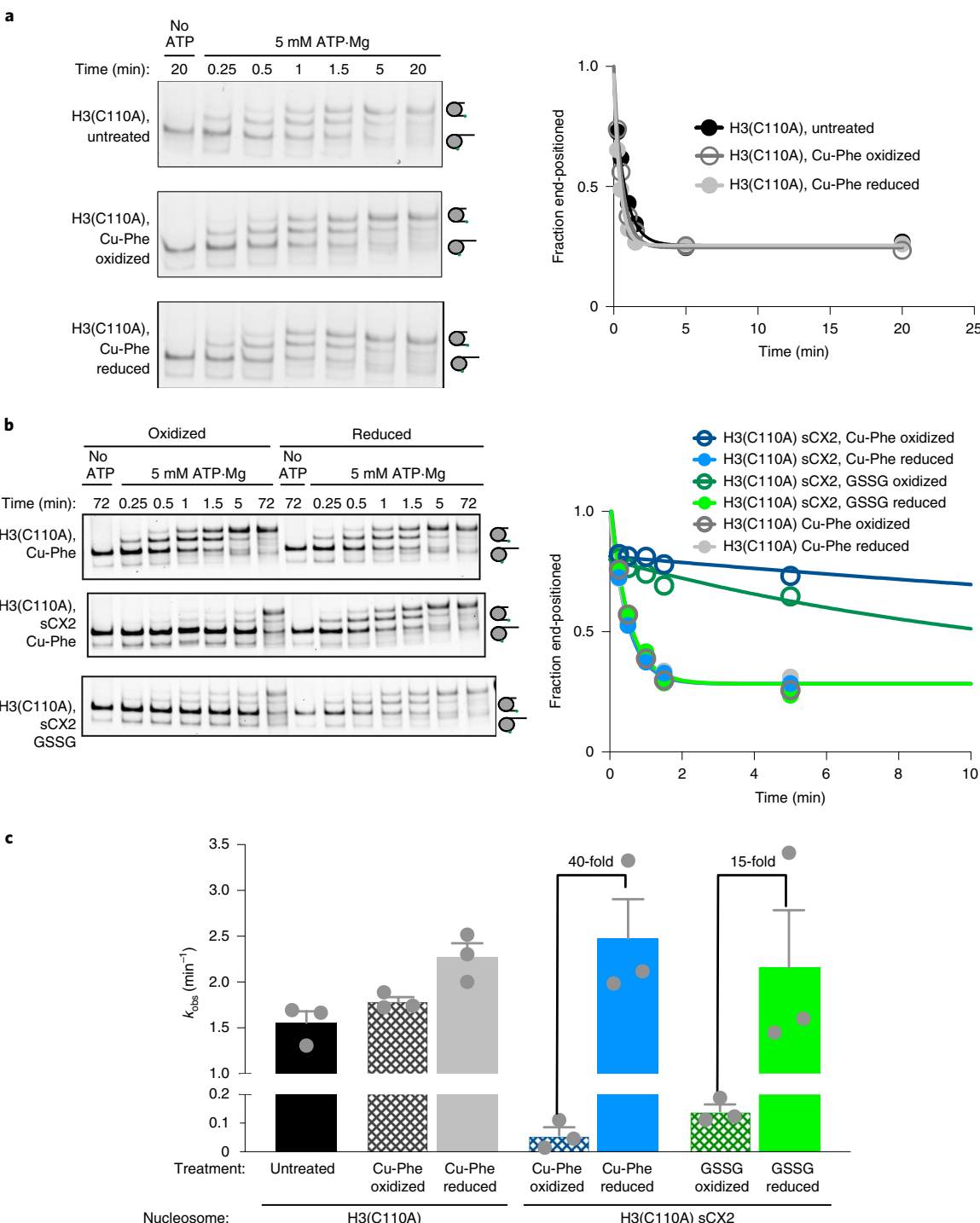


**Fig. 1 | Site-specific cysteine crosslinking, not general oxidative damage, inhibits remodeling regardless of oxidation method.** **a**, Treatment of the H3(C110A) histone octamer with Cu-Phe or GSSG does not affect nucleosome sliding by SNF2h. Left, native gel sliding assay with saturating concentrations of SNF2h (1 μM) with or without saturating ATP and 15 nM Cy3-labeled nucleosomes using the indicated histone octamer. Time points were quenched with excess ADP and plasmid DNA and resolved on a 6% (29:1 Bis) acrylamide gel. Higher migrating species are more centrally positioned nucleosomes. Right, quantification of the data shown on the left plotted as the fraction of end-positioned nucleosomes over time. The experiment was performed three times independently with similar results. **b**, Left, native gel remodeling assay as in **a**. Right, quantification of the data shown on the left plotted as the fraction of end-positioned nucleosomes over time, with the plot zoomed in to the first 10 min of the reaction to better evaluate fits. This experiment was performed three times independently with similar results. **c**, Mean observed rate constants ( $k_{obs}$ ) from three independent experiments. Data are mean  $\pm$  s.e.m. Uncropped images for **a** and **b** are available as source data and the numerical values plotted in the graphs are provided in Supplementary Table 1. In all figure panels, 'reduced' nucleosomes refer to nucleosomes that were assembled from octamers oxidized using the indicated method and then subjected to reducing conditions before nucleosome assembly.

nucleosome disassembly (Supplementary Figs. 1, 2). Reduction of either type of oxidized octamer fully restored SNF2h-dependent sliding of nucleosomes assembled from their respective octamers (Fig. 1b,c). To further test whether the oxidation-dependent effect on SNF2h-dependent sCX2 nucleosome remodeling is due to the formation of a disulfide bond, we also tested remodeling on nucleosomes assembled using oxidized H3(C110A) octamers containing single cysteines from the sCX2 cysteine pair that were purified by ultracentrifugation (Extended Data Fig. 2a). In this side-by-side experiment, SNF2h remodeled Cu-Phe oxidized H3(C110A) sCX2 nucleosomes around 30-fold slower than untreated H3(C110A) nucleosomes in line with our previous observations, whereas single-cysteine-containing nucleosomes were remodeled only approximately twofold slower. Oxidation-dependent remodeling defects were also observed with sub-saturating concentrations of enzyme (Extended Data Fig. 2b). These results indicate that non-specific oxidative damage to the octamer cannot explain the remodeling defects.

To determine whether any differences in the remodeling assay protocols could explain the discrepancies between the two studies, we repeated the remodeling reaction under the conditions used by Yan et al.<sup>4</sup>. Although the remodeling reactions were faster overall (Extended Data Fig. 2c), even under these conditions a disulfide bond between the sCX2 cysteine pair causes a >6-fold reduction in reaction rate (Extended Data Fig. 2c). Owing to the faster remodeling reaction, nucleosomes are already around 60% remodeled at the first time point that we are able to capture (0.3 min). As a result, the rate constant reported here for non-oxidized nucleosomes should be considered an underestimate and the sixfold defect should be considered a lower limit.

These results (summarized in Table 1) (1) rule out non-specific octamer oxidation causing inhibition of sliding; (2) reproduce the inhibitory effects seen by Sinha et al.<sup>1</sup> when the H3(L82C)-H4(V81C) disulfide bond is formed in an H3(C110A) nucleosome; and (3) show that this defect is reversible when the oxidized octamer is reduced before nucleosome assembly.

Notably, Yan et al.<sup>4</sup> tested the reversibility in a different manner than described above. Specifically, while their oxidation reaction was carried out in the context of an octamer, their reduction reaction was carried out in the context of a nucleosome. In our experience, reducing buried disulfides in the context of a fully assembled nucleosome is difficult, likely because the disulfide crosslink is less solvent-accessible in a nucleosome compared to an octamer. When we reduced crosslinked H3(C110A) sCX2 nucleosomes following the same protocol as Yan et al.<sup>4</sup> (treatment of crosslinked nucleosomes with 100 mM DTT at 37°C for 1 h), we found that SNF2h sliding activity was not restored, consistent with their report (Extended Data Fig. 3a). Although Yan et al.<sup>4</sup> showed that these conditions were sufficient to completely break the disulfide bond when assayed by non-reducing SDS-PAGE, we reasoned that if the sample was not buffer-exchanged to remove excess DTT before denaturation in the SDS-PAGE loading buffer, once-buried disulfides could become exposed upon denaturation and rapidly reduced by the residual DTT. This would cause an overestimation of the degree of reduction by SDS-PAGE. To test this possibility, we reduced H3(C110A) sCX2 crosslinked nucleosomes with 100 mM DTT for 1 h at 37°C and either directly added the sample to SDS loading buffer or quenched the residual DTT with five-fold excess *N*-ethyl maleimide before SDS treatment. Whereas in the unquenched sample the disulfide bond is completely reversed, quenching the sample before SDS treatment causes retention of the disulfide bond (Extended Data Fig. 3c). This retention cannot be explained by re-oxidation of the disulfide bond upon quenching as *N*-ethyl maleimide would also react with cysteine thiols, blocking the formation of new disulfide bonds. In addition, oxidation of the cysteines within octamers in the absence of catalysts such

as Cu-Phe or GSSG is extremely slow ( $\geq 48$  h)<sup>1</sup>. It is therefore possible that the apparent inability by Yan et al.<sup>4</sup> to reverse the nucleosome sliding defects associated with octamer crosslinking may have been due to an inability to completely reverse crosslinking in fully assembled nucleosomes, and that the reduction that they observe occurs while processing the samples for analysis by SDS-PAGE. The results underscore the importance of performing both oxidation and reduction reactions in the context of the histone octamer when attempting to generate or reverse crosslinks to investigate the role of histone dynamics.

In their Reply<sup>7</sup>, Chen and colleagues now propose that the disulfide bond may damage the integrity of the histone octamer, an argument that is different from their original hypothesis of non-specific oxidative damage. To support this claim, the authors provide data suggesting that the sCX2 disulfide crosslinked histone octamer has reduced stability. However, they do not provide evidence for reduced stability in the context of a nucleosome, which is the relevant substrate. We contend that the data that we present here tests whether the sCX2 disulfide bond affects nucleosome stability. Specifically, when comparing unremodeled nucleosomes assembled from oxidized and reduced sCX2 octamers, after incubation in reaction buffer with SNF2h for more than an hour, we observe similar levels of intact nucleosomes, suggesting no differences in the stability of the two samples (Fig. 1b and Supplementary Fig. 2a; see ‘no ATP’ lanes).

Notably, our results do not invalidate the other conclusions drawn in the article by Yan et al.<sup>4</sup> nor do they cast doubt on the quality of the structural data presented. Cryo-EM structures represent only a fraction of the states that can be reconstructed to high resolution. Lowly populated or highly dynamic states would likely be lost during the averaging required for high-resolution analysis. Consistent with this possibility, a recent cryo-EM study captured multiple stable ISWI-nucleosome states<sup>8</sup>. Whereas the highest resolution structures showed no clear evidence of conformational dynamics, lower resolution structures showed local reduction in the cryo-EM density that overlaps both with dynamic regions captured by NMR<sup>1</sup> and with the crosslinked residues tested here and in Sinha et al<sup>1</sup>. These results are consistent with SNF2h promoting the formation of an ensemble of highly dynamic conformations that cannot be directly visualized by cryo-EM averaging. As a consequence, the absence of a stable deformed histone octamer in the cryo-EM density reported by Yan et al.<sup>4</sup> is still fully compatible with the conclusion that dynamic histone deformation is important for nucleosome sliding.

In summary, we replicate our previous findings that restraining histone dynamics with disulfide crosslinks interferes with SNF2h-mediated nucleosome sliding. We further show that this finding is robust to the method of crosslinking and cannot be explained by non-specific oxidative damage to the nucleosome. The inability to replicate this finding by Yan et al.<sup>4</sup> might be due to the incomplete reduction of the disulfide bond in the context of the nucleosome. Overall, we contend that our results support an important role for histone octamer plasticity during SNF2h-mediated nucleosome sliding.

### Online content

Any methods, additional references, Nature Research reporting summaries, source data, extended data, supplementary information, acknowledgements, peer review information; details of author contributions and competing interests; and statements of data and code availability are available at <https://doi.org/10.1038/s41594-021-00620-7>.

Received: 5 March 2020; Accepted: 4 June 2021;  
Published online: 5 July 2021

**References**

1. Sinha, K. K., Gross, J. D. & Narlikar, G. J. Distortion of histone octamer core promotes nucleosome mobilization by a chromatin remodeler. *Science* **355**, eaaa3761 (2017).
2. Hada, A. et al. Histone octamer structure is altered early in ISWI2 ATP-dependent nucleosome remodeling. *Cell Rep.* **28**, 282–294 (2019).
3. Bilokapic, S., Strauss, M. & Halic, M. Structural rearrangements of the histone octamer translocate DNA. *Nat. Commun.* **9**, 1330 (2018).
4. Yan, L. et al. Structures of the ISWI–nucleosome complex reveal a conserved mechanism of chromatin remodeling. *Nat. Struct. Mol. Biol.* **26**, 258–266 (2019).
5. Ausio, J., Seger, D. & Eisenberg, H. Nucleosome core particle stability and conformational change. Effect of temperature, particle and NaCl concentrations, and crosslinking of histone H3 sulphhydryl groups. *J. Mol. Biol.* **176**, 77–104 (1984).
6. Sanulli, S. et al. HP1 reshapes nucleosome core to promote phase separation of heterochromatin. *Nature* **575**, 390–394 (2019).
7. Li, L., Yan, L. & Chen, Z. Reply to: Histone dynamics play a critical role in SNF2h-mediated nucleosome sliding. *Nat. Struct. Mol. Biol.* <https://doi.org/10.1038/s41594-021-00621-6> (2021).
8. Armache, J. P. et al. Cryo-EM structures of remodeler-nucleosome intermediates suggest allosteric control through the nucleosome. *Elife* **18**, e46057 (2019).

**Publisher's note** Springer Nature remains neutral with regard to jurisdictional claims in published maps and institutional affiliations.

© The Author(s), under exclusive licence to Springer Nature America, Inc. 2021

**Methods**

A detailed description of the methods is available in Supplementary Note 1.

**Reporting Summary.** Further information on research design is available in the Nature Research Reporting Summary linked to this article.

**Data availability**

All relevant data are included in the paper and its Supplementary Information. Uncropped images of gels and blots are provided as source data, and numerical values plotted in the graphs are available in Supplementary Table 1. Source data are provided with this paper.

**Acknowledgements**

We thank K. Sinha for help generating the disulfide-crosslinked nucleosome; J. Tretyakova for preparing histones; S. Sanulli, J. Gross, J. Lobel and Y. Cheng for feedback in preparing this manuscript; and all members of the Narlikar laboratory for discussions. This work was supported by a grant from the NIH to G.J.N. (R35GM127020) and an NSF predoctoral and UCSF discovery fellowship to N.G.

**Author contributions**

N.G. conceived and performed the experiments, performed data analysis and wrote and edited the original draft of the manuscript. G.J.N. helped to design experiments, contributed to the writing and editing of the manuscript and supervised the overall project.

**Competing interests**

The authors declare no competing interests.

**Additional information**

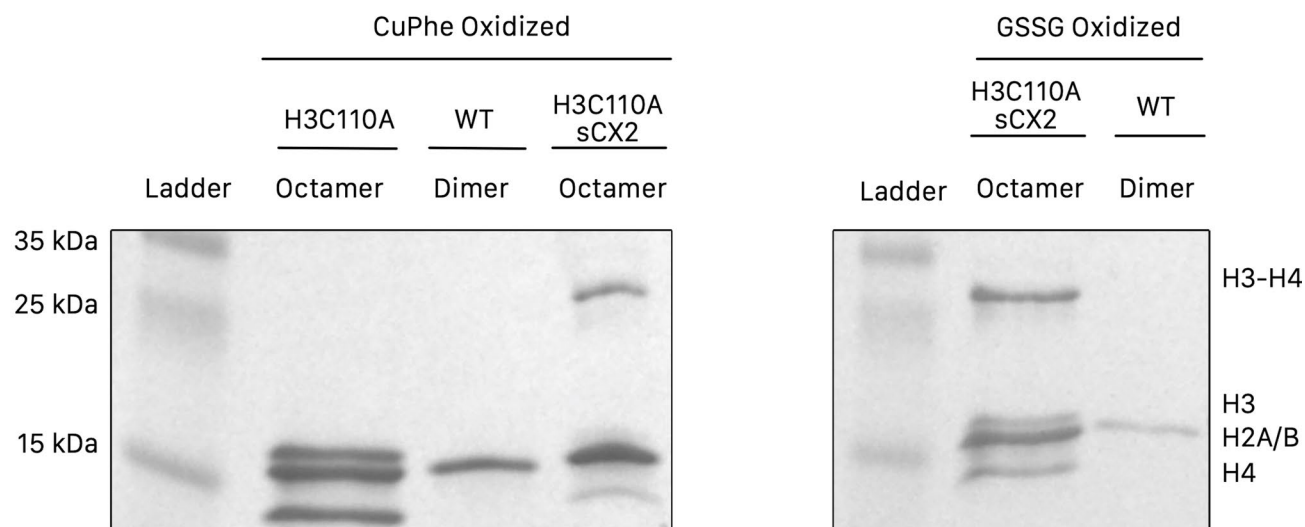
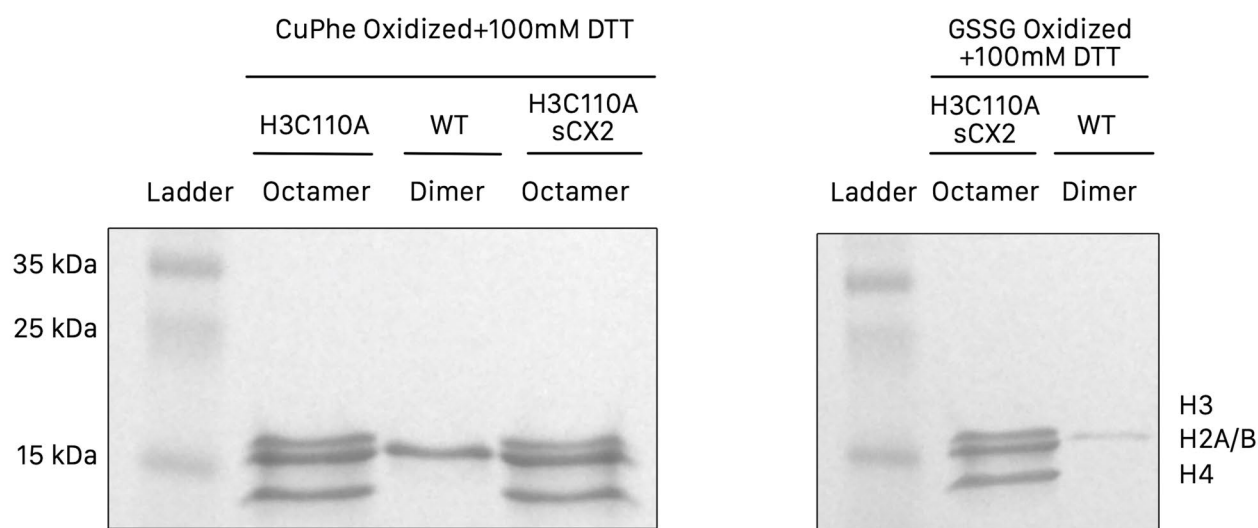
**Extended data** is available for this paper at <https://doi.org/10.1038/s41594-021-00620-7>.

**Supplementary information** The online version contains supplementary material available at <https://doi.org/10.1038/s41594-021-00620-7>.

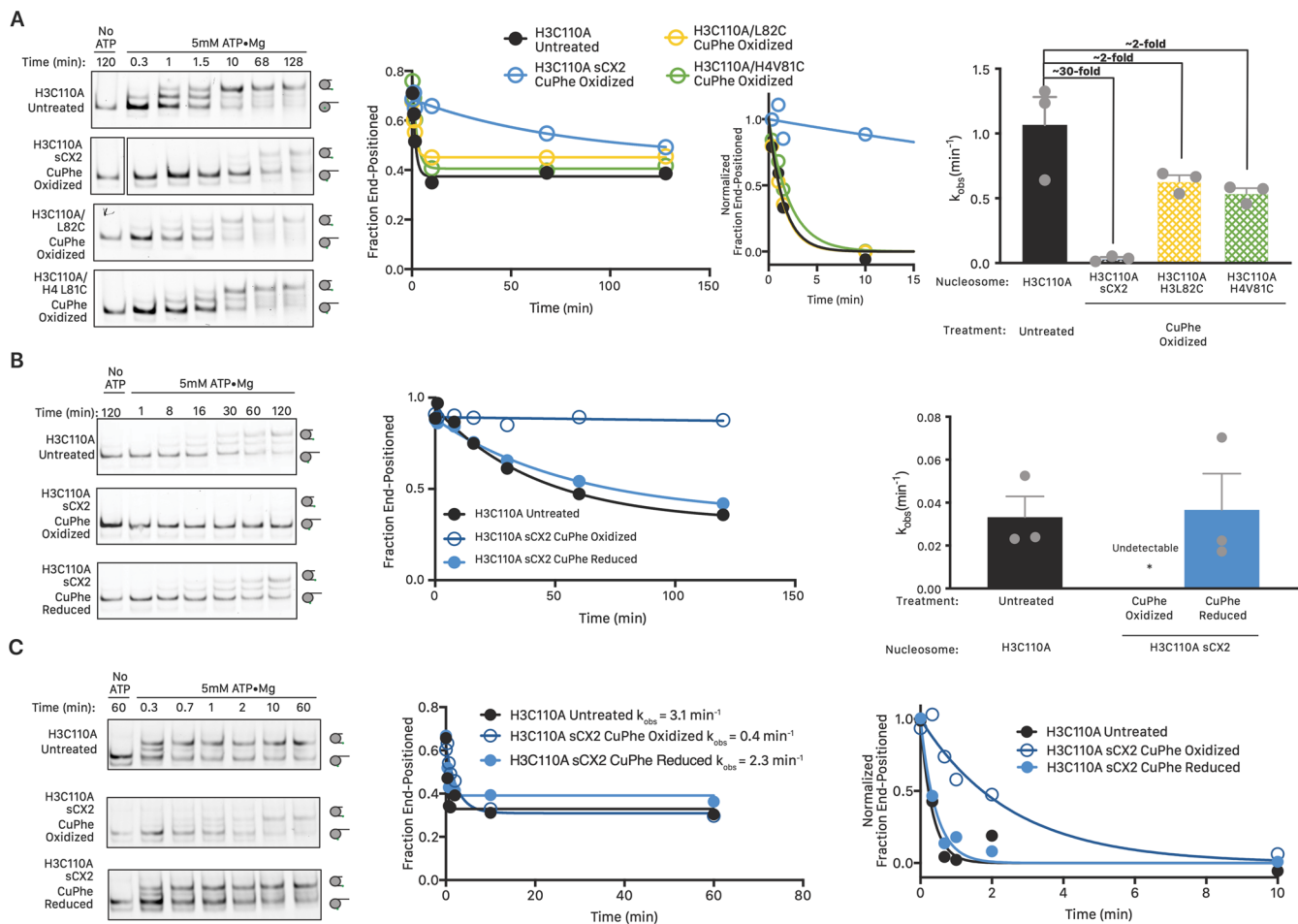
**Correspondence and requests for materials** should be addressed to G.J.N.

**Peer review information** Anke Sparmann was the primary editor on this article and managed its editorial process and peer review in collaboration with the rest of the editorial team.

**Reprints and permissions information** is available at [www.nature.com/reprints](http://www.nature.com/reprints).

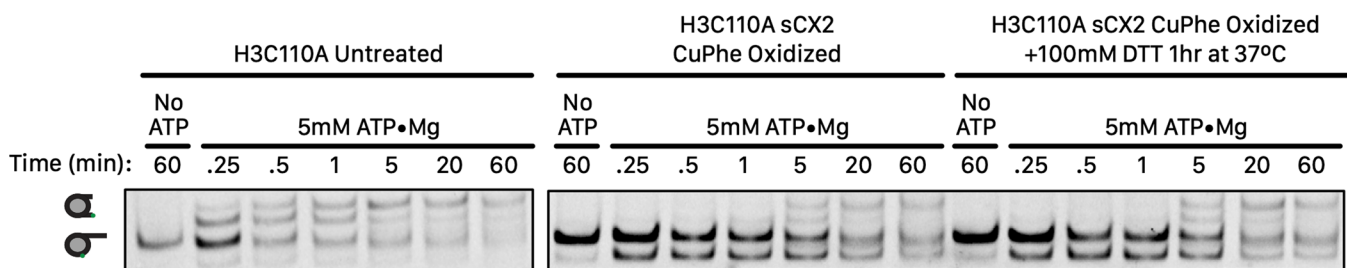
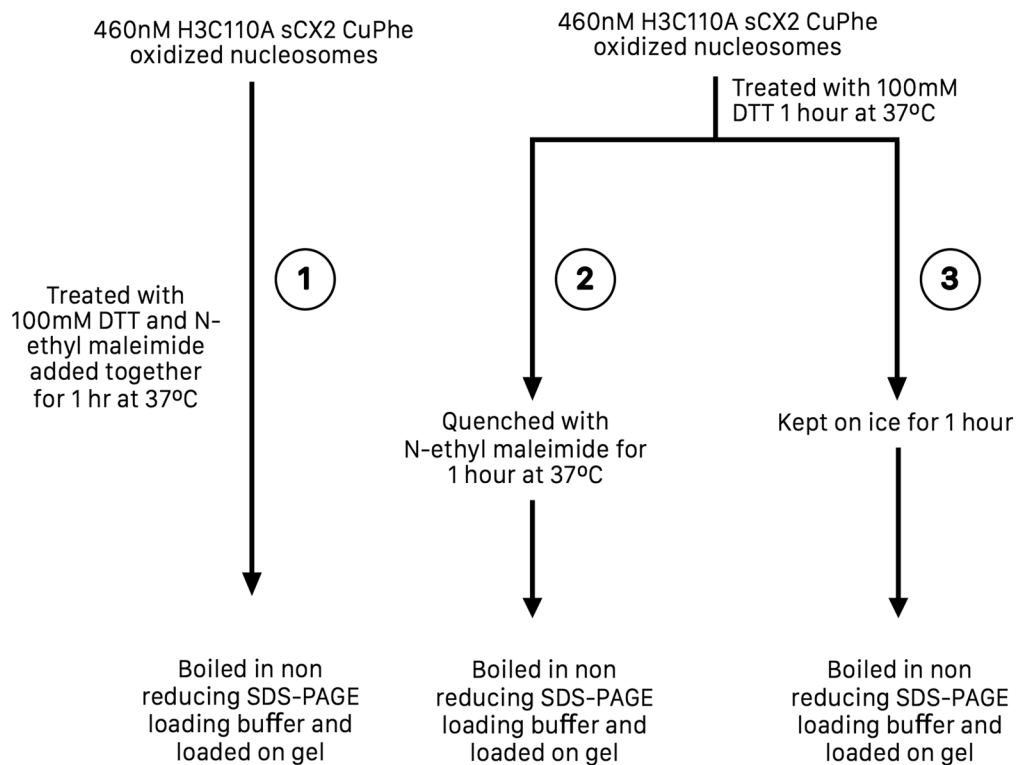
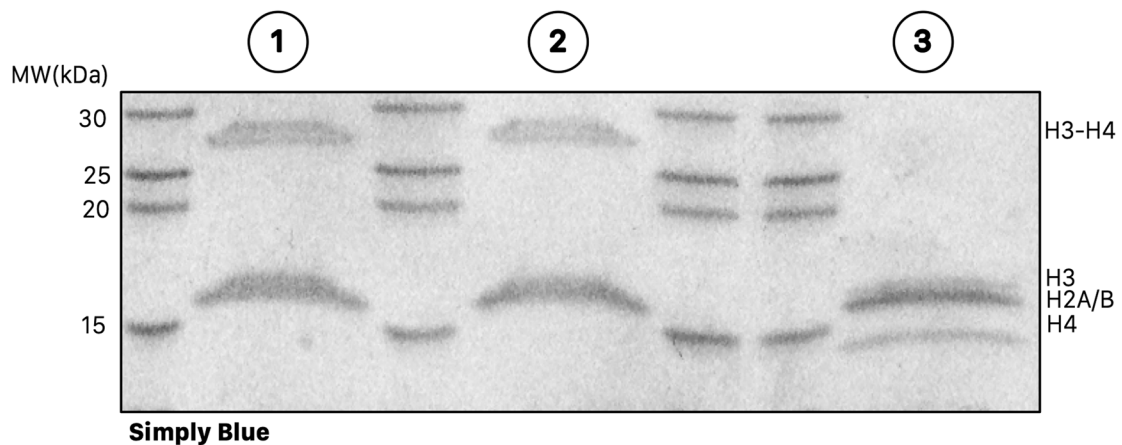
**A****B**

**Extended Data Fig. 1 | Preparation of crosslinked and reduced histone octamers.** SDS-PAGE gels of *Xenopus laevis* of histones used to prepare all nucleosomes in this study. **(a)** Wild type (WT) Histone H2A-H2B dimer as well as H3C110A histone octamer and H3C110A sCX2 (H3 L82C, H4 V81C) histone octamer oxidized using copper phenanthroline (CuPhe) or oxidized glutathione (GSSG). **(b)** The same samples used in (A) treated with 100 mM DTT in order to reduce the disulfide bond. Uncropped images are available as source data files. SDS-PAGE analysis was only performed once for all samples.



#### Extended Data Fig. 2 | Remodeling of oxidized nucleosomes is slowed specifically due to disulfide bond formation and is robust to remodeling conditions.

(a) Left. Native gel remodeling assay with saturating SNF2h (1  $\mu\text{M}$ ), saturating ATP, and 15 nM cy3-nucleosomes as in Fig. 1. Middle. Quantification of the experiment at the left including a plot of all time points; and for ease of comparison a plot of the first 15 minutes of the reaction normalized to the best-fit parameters for YO and plateau. This experiment was performed 3 times with similar results. Right. Mean observed rate constants ( $k_{obs}$ ) from 3 independent experiments. Error bars reflect the standard error of the mean (SEM). (b) Left. Native gel remodeling assay with sub-saturating SNF2h (50 nM), saturating ATP, and 15 nM cy3-nucleosomes as in Fig. 1. Middle. Quantification of the experiment on the left. This experiment was performed 3 times with similar results. Right. Mean and SEM of the observed rate constants ( $k_{obs}$ ) from 3 independent experiments. The asterisk denotes that the rate constant for the oxidized reaction condition was too slow to reliably quantify with the time points taken. (C) Left. Native gel remodeling assay under the conditions of Yan et al. 2 using 50 nM SNF2h, saturating ATP, and 15 nM cy3-nucleosomes. Remodeling overall is substantially faster likely because of the different conditions used (higher temperature, lower salt concentration, the absence of .02% (v/v) NP40, and the presence of 0.1 mg/mL BSA). Middle. Quantification of the gel on the left along with the indicated observed rate constants. This experiment was performed once. Right. Time courses shown in the middle panel normalized to the best fit parameters for YO and Plateau of the exponential decay and zoomed in to the first 10 minutes of the reaction to better evaluate the fits. Uncropped images for panels A-C are available in Source Data and values obtained in quantifications are in Supplementary Table 1.

**A****B****C**

Extended Data Fig. 3 | See next page for caption.

**Extended Data Fig. 3 | Disulfide reduction is impaired in the context of the nucleosome.** (a) Native gel remodeling assay with saturating SNF2h (1 μM), saturating ATP, and 15 nM cy3-nucleosomes as in Fig. 1. Nucleosomes containing the oxidized sCX2 bonds were generated by oxidizing the H3C110A sCX2 octamer using CuPhe, and then assembling nucleosomes. Treatment of these nucleosomes with excess DTT as in Yan et al. fails to reverse the remodeling defect. (b) Scheme for the samples run in C. Nucleosomes treated with DTT were either directly added to non-reducing SDS-PAGE loading buffer or quenched with 500 mM N-Ethyl Maleimide freshly dissolved in DMSO (final [DMSO] ≈ 10% (v/v)). Additionally, a condition where N-Ethyl Maleimide and DTT were added simultaneously is included to evaluate the efficacy of the quench. (c) SDS-PAGE of samples treated as in B. Samples with reducing agent quenched prior to running on the gel are near-completely oxidized. The experiments shown here were performed once.

## Reporting Summary

Nature Research wishes to improve the reproducibility of the work that we publish. This form provides structure for consistency and transparency in reporting. For further information on Nature Research policies, see our [Editorial Policies](#) and the [Editorial Policy Checklist](#).

### Statistics

For all statistical analyses, confirm that the following items are present in the figure legend, table legend, main text, or Methods section.

n/a Confirmed

- The exact sample size ( $n$ ) for each experimental group/condition, given as a discrete number and unit of measurement
- A statement on whether measurements were taken from distinct samples or whether the same sample was measured repeatedly
- The statistical test(s) used AND whether they are one- or two-sided  
*Only common tests should be described solely by name; describe more complex techniques in the Methods section.*
- A description of all covariates tested
- A description of any assumptions or corrections, such as tests of normality and adjustment for multiple comparisons
- A full description of the statistical parameters including central tendency (e.g. means) or other basic estimates (e.g. regression coefficient) AND variation (e.g. standard deviation) or associated estimates of uncertainty (e.g. confidence intervals)
- For null hypothesis testing, the test statistic (e.g.  $F$ ,  $t$ ,  $r$ ) with confidence intervals, effect sizes, degrees of freedom and  $P$  value noted  
*Give P values as exact values whenever suitable.*
- For Bayesian analysis, information on the choice of priors and Markov chain Monte Carlo settings
- For hierarchical and complex designs, identification of the appropriate level for tests and full reporting of outcomes
- Estimates of effect sizes (e.g. Cohen's  $d$ , Pearson's  $r$ ), indicating how they were calculated

*Our web collection on [statistics for biologists](#) contains articles on many of the points above.*

### Software and code

Policy information about [availability of computer code](#)

Data collection Gel images were collected using the amersham FLA 9500 typhoon control software

Data analysis Gel images were quantified using FIJI (Imagej version 2.1.0/1/53c) and fit using GraphPad Prism 7

For manuscripts utilizing custom algorithms or software that are central to the research but not yet described in published literature, software must be made available to editors and reviewers. We strongly encourage code deposition in a community repository (e.g. GitHub). See the Nature Research [guidelines for submitting code & software](#) for further information.

### Data

Policy information about [availability of data](#)

All manuscripts must include a [data availability statement](#). This statement should provide the following information, where applicable:

- Accession codes, unique identifiers, or web links for publicly available datasets
- A list of figures that have associated raw data
- A description of any restrictions on data availability

All relevant data are included in the paper and its supplementary information files. Uncropped images of gels are provided as source data and numerical values plotted in the graphs are available in Supplementary Table 1.

# Field-specific reporting

Please select the one below that is the best fit for your research. If you are not sure, read the appropriate sections before making your selection.

- Life sciences       Behavioural & social sciences       Ecological, evolutionary & environmental sciences

For a reference copy of the document with all sections, see [nature.com/documents/nr-reporting-summary-flat.pdf](https://nature.com/documents/nr-reporting-summary-flat.pdf)

## Life sciences study design

All studies must disclose on these points even when the disclosure is negative.

Sample size	Three replicates were performed as is generally accepted for quantitative biochemical experiments.
Data exclusions	No data were excluded from this study
Replication	All experiments were performed for the indicated number of replicates. All replicates reproduced the original findings
Randomization	Samples were assigned to groups based on their method of preparation and no randomization was necessary
Blinding	Samples were not blinded as knowledge of the samples tested by the experimenter should not influence biochemical experiments

## Reporting for specific materials, systems and methods

We require information from authors about some types of materials, experimental systems and methods used in many studies. Here, indicate whether each material, system or method listed is relevant to your study. If you are not sure if a list item applies to your research, read the appropriate section before selecting a response.

Materials & experimental systems		Methods	
n/a	Involved in the study	n/a	Involved in the study
<input checked="" type="checkbox"/>	<input type="checkbox"/> Antibodies	<input checked="" type="checkbox"/>	<input type="checkbox"/> ChIP-seq
<input checked="" type="checkbox"/>	<input type="checkbox"/> Eukaryotic cell lines	<input checked="" type="checkbox"/>	<input type="checkbox"/> Flow cytometry
<input checked="" type="checkbox"/>	<input type="checkbox"/> Palaeontology and archaeology	<input checked="" type="checkbox"/>	<input type="checkbox"/> MRI-based neuroimaging
<input checked="" type="checkbox"/>	<input type="checkbox"/> Animals and other organisms		
<input checked="" type="checkbox"/>	<input type="checkbox"/> Human research participants		
<input checked="" type="checkbox"/>	<input type="checkbox"/> Clinical data		
<input checked="" type="checkbox"/>	<input type="checkbox"/> Dual use research of concern		